NUCLEAR ENGINEERING AND TECHNOLOGY
ISSN / eISSN 1738-5733
Publisher KOREAN NUCLEAR SOC,
NUTOPIA BLDG, 342-1 JANGDAE-DONG,
DAEJEON, SOUTH KOREA,
Volume 26-Issue 1-(2026)
DOI:https://doi.org/10.65281/734537

OPEN ACCESS

Integrated QSAR, DFT and Docking Study of Hydantoin Derivatives for Anti-Epileptic and Plasmin Inhibition

Lazhar BOUCHLALEG [1], ZIDANI Sara [2], BAIRA Fayçal [3], Yamina Benkrima [4]

[1] Innovation Laboratory of Construction Eco-design and Geny Seismic (LICEGS Laboratory), Faculty of Technology, University of Batna 2, Batna 05000, Algeria
Email: l.bouchlaleg@univ-batna2.dz ; Orcid : 0009-0009-3680-9761
[2]university of Batna Departement of Food Technology, laboratory of Food Science (lSa), institute of veterinary and agricultural Sciences, 1 hadjlakhdar, alleys may 19 Biskra avenue, Batna, 05000, Algeria
Email: sara.zidani@univ-batna.dz ; Orcid: 0009-0004-3604-2437
[3] university of Batna 2, Faculty of Technology, Department oF Sciences and Technology, alleys 53, constantine avenue. Fésdis, Batna 05078, Algeria
Email: f.baira@univ-batna2.dz ; 0009-0008-0869-8614
[4] MPMMDMEER Laboratory, ENS Ouargla, 30000 Ouargla, Algeria
Email: benkrima.yamina@ens-ouargla.dz ; Orcid: 0000-0002-7089-7904

Received: 11 November 2025 ; Accepted: 25 March 2026

Abstract

Hydantoin and thiohydantoin derivatives constitute an important family of nitrogen-based heterocyclic compounds that have attracted considerable attention because of their diverse pharmacological properties, including anticonvulsant, antimicrobial, anticancer, and enzyme inhibitory activities. In this investigation, an integrated computational strategy combining QSAR modeling, quantum chemical calculations, and molecular docking was employed to analyze the structural factors influencing their biological behavior.Eighteen hydantoin analogues reported as plasmin inhibitors were selected for the study. QSAR analysis using multiple linear regression demonstrated that molecular descriptors associated with surface area, molar refractivity, and polarizability positively affect inhibitory activity, whereas excessive molecular volume and lipophilicity contribute negatively.

Quantum chemical studies performed using HF and DFT approaches generated structural and electronic parameters that were in close agreement with experimental observations, supporting the reliability of the theoretical methodology. The presence of substituents such as methyl and chloro groups was shown to markedly influence charge distribution and molecular reactivity.Docking experiments carried out on the Metabotropic glutamate receptor 1 (GRM1, PDB ID: 5KZQ) revealed favorable ligand–receptor interactions, with binding affinities reaching approximately −9.5 kcal/mol.

The stability of the complexes was mainly attributed to hydrogen-bond formation and hydrophobic interactions within the receptor active pocket.

The combined results suggest that hydantoin-based molecules represent promising scaffolds for plasmin inhibition and potential anti-epileptic applications. This work provides valuable molecular insights that may support the rational development of new therapeutic agents.

Keywords: Hydantoin derivatives; QSAR modeling; Molecular docking; Plasmin inhibition; Epilepsy; GRM1 receptor; Rational drug design.

1. INTRODUCTION

Five-membered nitrogen-containing heterocycles, particularly hydantoins and thiohydantoins, play a significant role in medicinal chemistry because of their wide range of biological and pharmacological applications. Their core structure, derived from the 2,4-imidazolidinedione nucleus, offers several positions suitable for chemical modification, allowing optimization of physicochemical and therapeutic properties.Among the best-known hydantoin-based drugs, Phenytoin remains a classical anticonvulsant widely used in the treatment of epilepsy[5,6]. Structural alterations of the hydantoin ring, especially oxygen-to-sulfur substitution yielding thiohydantoins, can substantially modify electronic distribution, lipophilicity, and biological performance.In addition to their anticonvulsant potential, hydantoin derivatives have emerged as attractive candidates for plasmin inhibition. Plasmin, a serine protease involved in fibrinolysis, tumor progression, and metastasis, represents an important therapeutic target in several pathological conditions[10,11]. Consequently, the design of effective plasmin inhibitors has become an active area of pharmaceutical research[1, 2, 36].Recent studies have also emphasized the critical role of glutamatergic neurotransmission in neurological disorders. In this context, the Metabotropic glutamate receptor 1 (GRM1) has attracted considerable interest because of its involvement in synaptic regulation and neuronal excitability associated with epilepsy.The rapid evolution of computational chemistry has greatly facilitated modern drug discovery. Computational techniques such as quantitative structure–activity relationship (QSAR) analysis, density functional theory (DFT), Hartree–Fock (HF) calculations, and molecular docking provide complementary information regarding molecular geometry, electronic structure, and ligand–target interactions.Therefore, the present study employs an integrated in silico methodology combining QSAR modeling, quantum chemical investigations, and docking simulations to better understand the structure–activity relationships of hydantoin derivatives and identify promising candidates with potential plasmin inhibitory and anti-epileptic properties[26,27].

2. MATERIALS AND METHODS

A dataset composed of eighteen hydantoin derivatives with experimentally determined plasmin inhibitory activities expressed as pIC_{50} values was collected from previously published studies.

The molecular structures were initially constructed and subjected to geometry pre-optimization using molecular mechanics (MM+) methods. Semi-empirical optimization was subsequently performed with the PM3 approach to obtain energetically stable conformations. Higher-level quantum chemical calculations were then carried out using both Hartree–Fock (HF) and density functional theory (DFT) methods, particularly the B3LYP functional combined with suitable basis sets, in order to generate accurate structural and electronic descriptors[12,13].

Several physicochemical parameters were calculated for each derivative, including molecular surface area, molecular volume, lipophilicity (log P), hydration energy, molar refractivity, and polarizability. These

descriptors were selected because of their relevance to steric, hydrophobic, and electronic molecular properties.

To establish quantitative relationships between molecular structure and biological activity, multiple linear regression (MLR) analysis was applied. The statistical quality and predictive reliability of the developed QSAR models were evaluated using parameters such as the coefficient of determination (R^2), Fisher statistic (F), standard error (SE), and leave-one-out (LOO) cross-validation procedures[13, 18]

In addition, vibrational frequency calculations were performed and compared with available experimental spectra to validate the theoretical models and confirm the accuracy of the optimized geometries.

Molecular docking studies were conducted using AutoDock Vina against the Metabotropic glutamate receptor 1 (PDB ID: 5KZQ). The resulting ligand–receptor complexes were analyzed according to hydrogen bonding, hydrophobic interactions, π–π stacking, and electrostatic contacts within the active site[33, 35].

2.1 Dataset for QSAR Investigation

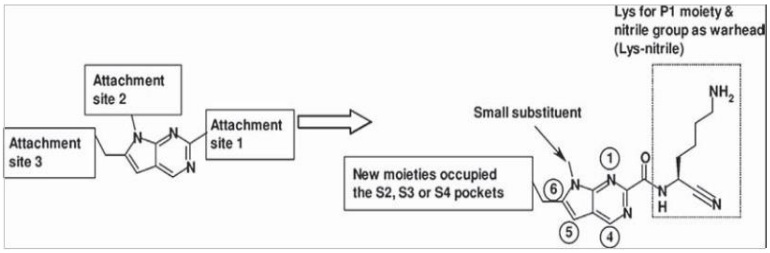

Fig. 1. Schematic outline for developing new chemotype of plasmin inhibitors.

The present work focused on a structurally diverse series of hydantoin derivatives reported as plasmin inhibitors. The molecular design strategy aimed to optimize interactions within the catalytic binding pocket of the target enzyme through systematic scaffold functionalization. Different substitution positions were introduced around the heterocyclic core in order to modulate steric, hydrophobic, and electronic characteristics while maintaining favorable molecular recognition.The designed compounds were expected to interact efficiently with the S2–S4 sub-sites of plasmin through a combination of hydrogen bonding, electrostatic attractions, and hydrophobic contacts[19]. A lysine fragment positioned at the P1 site was incorporated to improve enzyme recognition, whereas the nitrile functionality served as an electrophilic center capable of reversible covalent interaction with the catalytic serine residue. This rational design approach combines selective pocket recognition with optimized steric complementarity to improve inhibitory potency and selectivity[17, 18].

Structure–Physicochemical Property Relationships

At the beginning of the investigation, several important physicochemical descriptors were analyzed for the eighteen hydantoin derivatives in order to better understand the molecular factors influencing plasmin inhibitory activity. These descriptors were selected to represent steric, hydrophobic, and electronic molecular contributions.Molecular dimensions were characterized through molecular volume and surface area, corresponding to the spatial region enclosed by the Van der Waals surface of each compound[15, 16]. These parameters provide useful information regarding steric accessibility and the capacity of the ligands to fit into biological receptor cavities.Polarizability was considered an essential electronic descriptor because it reflects the ability of the electronic cloud to undergo deformation under an external electric field. Highly polarizable molecules generally exhibit stronger intermolecular

interactions, particularly dispersion forces, which may enhance ligand–target affinity.Molar refractivity, which is closely associated with molecular size and electronic distribution, was also evaluated as an additional steric and electronic descriptor. Variations observed among the compounds were consistent with differences in substituent size and chemical nature. Molecules containing bulky substituents exhibited increased refractivity and polarizability values, indicating greater electronic flexibility, whereas smaller derivatives showed more compact electronic distributions.Hydration energy analysis revealed that increasing hydrophobicity leads to reduced solvation effects[17,21]. Since molecular recognition in biological systems largely depends on reversible interactions with surrounding water molecules, hydration behavior represents an important determinant of biological performance.The hydrogen bond donor (HBD) and hydrogen bond acceptor (HBA) capacities also varied among the investigated compounds. Molecules possessing larger numbers of donor and acceptor groups are generally capable of forming stronger and more stable intermolecular interactions with biological targets.Lipophilicity, represented by the log P parameter, was identified as a major factor influencing pharmacokinetic behavior. Moderate lipophilicity is usually associated with an appropriate compromise between membrane permeability and aqueous solubility. Excessive lipophilic character may reduce solubility, whereas highly hydrophilic molecules may exhibit insufficient membrane penetration.Overall, the obtained results indicate that biological activity strongly depends on achieving a balanced combination of molecular size, polarity, hydrogen-bonding capability, and lipophilic character within the hydantoin scaffold[1,10].

Quantitative Structure–Activity Relationship (QSAR) Analysis

In the second phase of the study, quantitative structure–activity relationship analysis was employed to investigate the relationship between molecular descriptors and plasmin inhibitory activity of the hydantoin derivatives. Multiple linear regression (MLR) methodology was applied to the dataset composed of eighteen compounds using the previously calculated physicochemical parameters as independent variables[14].The development of a reliable QSAR model requires both structural diversity and the selection of meaningful molecular descriptors capable of accurately representing steric, hydrophobic, and electronic effects. Since molecular descriptors are numerical representations of chemical properties, identifying the most relevant subset is essential to improve model robustness and predictive capacity.To achieve this objective, Pearson correlation analysis was performed using SPSS Statistics [19]. This statistical screening procedure enabled the identification of the most significant descriptors, which were subsequently incorporated into the final MLR-QSAR model for biological activity prediction.

3. RESULTS AND DISCUSSION

3.1 QSAR Analysis of Hydantoin Derivatives as Plasmin Inhibitors

The QSAR investigation demonstrated that the inhibitory potency of hydantoin derivatives toward plasmin is strongly governed by steric, hydrophobic, and electronic molecular characteristics.

Multiple linear regression analysis produced a statistically reliable predictive equation correlating the experimental pIC_{50} values with selected molecular descriptors.The developed QSAR relationship is represented by:

$$pIC50=5.023+0.024S-0.025V+0.46RF+0.147Pol-0.080logP$$

$$pIC_{50}=5.023+0.024S-0.025V+0.46RF+0.147Pol-0.080\log$$

$$PpIC50 \quad =5.023+0.024S-0.025V+0.46RF+0.147Pol-0.080logP$$

where:*S* corresponds to molecular surface area, *V* represents molecular volume, *RF* denotes molar refractivity, *Pol* indicates polarizability, *log P* represents lipophilicity.

The positive coefficients associated with surface area, refractivity, and polarizability indicate that increased steric exposure and enhanced electronic flexibility favor stronger ligand–enzyme interactions. In contrast, excessive molecular volume may negatively influence activity because of steric hindrance within the receptor active site[7, 8].

Likewise, highly lipophilic derivatives may exhibit reduced biological efficiency due to unfavorable balance between solubility and target accessibility[1, 3].

These observations suggest that efficient plasmin inhibitors should possess moderate molecular dimensions, sufficient polarizability, balanced hydrophilic/lipophilic properties, and appropriate surface area capable of promoting intermolecular recognition. Consequently, suitable substitution around the hydantoin nucleus can significantly modulate inhibitory activity and pharmacological performance continue[4,6].

3.2 Screening of Synthesized Compounds and ADME EVALUATION

The physicochemical and pharmacokinetic properties of the synthesized hydantoin derivatives were further evaluated using the SwissADME platform. Important molecular parameters including molecular weight, oral bioavailability, skin permeability, and blood–brain barrier (BBB) permeability were analyzed in order to estimate the drug-likeness and pharmacokinetic behavior of the investigated compounds.The obtained ADME profiles indicated that most compounds possess physicochemical characteristics compatible with acceptable pharmacological performance. Moderate molecular weight and balanced lipophilicity were found to contribute positively to membrane permeability and oral bioavailability[28, 42]. In addition, several compounds demonstrated the potential to cross the blood–brain barrier, which is an important requirement for anti-epileptic agents targeting the central nervous system.The IUPAC nomenclature and structural characteristics of representative compounds are summarized in the corresponding tables and molecular structure figures.

Table-1: List of Compounds and their IUPAC name

Compound number	IUPAC name
A	*3-[(2,4-dioxo-8-(3-chlorophenyloyl)-1,3,8-triazaspiro[4.6]undec-3- yl)methyl]benzonitrile*
B	*3-[(2,4-dioxo-8-(3-fluorophenyloyl)-1,3,8- triazaspiro[4.6]undec-3-yl)methyl]benzonitrile*

Two-dimensional Structure of the Compounds

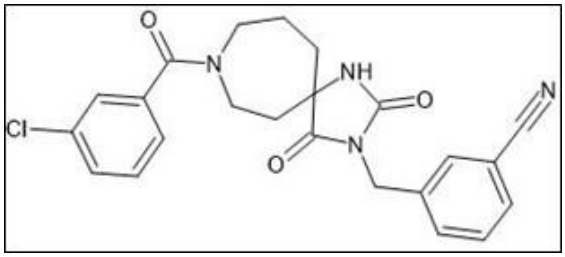

Figure 1: 3-[(2,4-dioxo-8-(3-chlorophenyloyl)-1,3,8- triazaspiro[4.6]undec-3-yl)methyl]benzonitrile

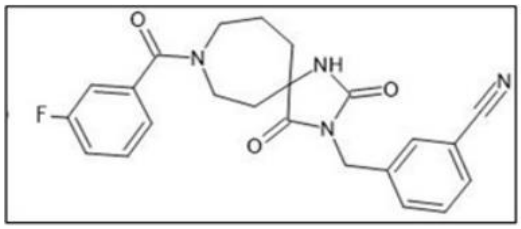

Figure 2: 3-[(2,4-dioxo-8-(3-fluorophenyloyl)-1,3,8- triazaspiro [4.6]undec-3- yl)methyl]benzonitrile

3.3 Geometry Optimization of Hydantoin and Thiohydantoin Derivatives

Geometry optimization studies were carried out using both Hartree–Fock (HF) and density functional theory (DFT) methods. The calculated structural parameters showed good agreement with available experimental measurements, confirming the reliability of the theoretical approach employed in this work.The substitution of oxygen atoms by sulfur within the heterocyclic ring significantly influenced molecular geometry and electronic properties. In particular, sulfur-containing derivatives exhibited longer bond lengths, increased molecular softness, and higher polarizability values. These modifications are expected to improve intermolecular interactions with biological targets by enhancing electronic flexibility.Frontier molecular orbital analysis demonstrated that molecular reactivity is strongly related to the HOMO–LUMO energy gap. Molecules possessing smaller energy gaps generally showed higher chemical reactivity and greater interaction potential. Electron-withdrawing substituents tended to favor electrophilic behavior, whereas electron-donating groups promoted nucleophilic character[29, 42].Vibrational frequency calculations confirmed the presence of characteristic absorption bands associated with N–H, C=O, and C=S functional groups. The

theoretical spectra were consistent with experimental observations, supporting the validity of the optimized molecular structures.Overall, the combined quantum chemical and physicochemical analyses revealed that parameters such as molecular size, hydrogen-bonding capability, polarizability, and lipophilicity play essential roles in determining plasmin inhibitory activity and receptor binding efficiency. Docking investigations additionally confirmed favorable interactions with the GRM1 receptor, highlighting the potential anti-epileptic properties of the studied compounds.The three-dimensional conformations and atom numbering systems adopted for hydantoin derivatives were generated using GaussView 09[1,2,3].

Conformation 3D of molecular structure and atom numbering adopted in this study for

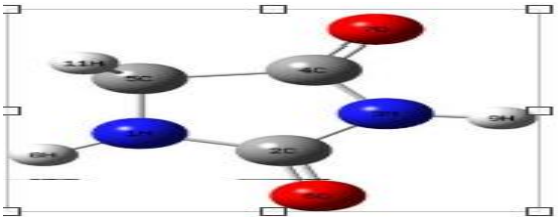

hydantoin (GaussView 09)

Experimental and calculated values of bond lengths and bond angles of Hydantoin

Parameters	Exp.	ab initio/HF			DFT(B3LYP)		
Bond Length (A°)	[22]	6-31G+(d,p)	6-31G++(d,p)	6-311G++(d,p)	6-31G+(d,p)	6-31G++(d,p)	6-311G++(d,p)
C2-O6	1,222	1,19183	1,19188	1,18516	1,21581	1,21583	1,20705
C2-N1	1,371	1,3556	1,35556	1,35568	1,36382	1,36379	1,36137
C2-N3	1,393	1,3899	1,38991	1,39025	1,40388	1,40390	1,40267
N3-C4	1,367	1,3662	1,3662	1,36635	1,36987	1,36987	1,36775
C4-O7	1,225	1,18847	1,18850	1,18216	1,21483	1,21482	1,20641
C4-C5	1,460	1,5218	1,52188	1,52148	1,51962	1,51967	1,51714
C5-N1	1,457	1,4433	1,44329	1,44259	1,43253	1,43253	1,43006
Bond angle(°)							
O6-C2-N1	128,2	128,3769	128,373	128,438	128,646	128,649	128,752
O6-C2-N3	124,4	125,744	125,745	125,761	126,085	126,083	126,115
N3-C2-N1	107,4	105,879	105,883	105,801	105,269	105,268	105,133
C4-N3-C2	111,67	113,309	113,310	113,406	113,430	113,432	113,578
O7-C4-C5	125,3	127,070	127,075	127,089	127,121	127,120	127,125
C5-C4-N3	106,8	105,770	105,768	105,655	105,259	105,257	105,117
N1-C5-C4	104,7	101,820	101,823	101,919	102,843	102,842	102,926
C2-N1-C5	109,4	113,221	113,217	113,219	113,199	113,202	113,246
Dihedral angles(°)							
C5-N1-C2-N2	4,1	4,5	4,6	5,4	4,0	4,0	3,0
N1-C2-N2-C4	6,7	3,6	3,7	4,3	1,9	1,9	3,0
O2-C2-N1-C5	176,1	179,985	179,984	176,984	179,978	179,978	176,979
O4-C4-C5-N1	176,0	179,989	179,991	179,985	176,0	179,987	179,987

Experimental and calculated vibrational spectra of hydantoin

Mode N°	Symmetry	EXP. IR [24]	ab- initio/HF			DFT(B3LYP)			Assignment
			6-31G+(d,p)	6-31G++ (d,p)	6-311G++ (d,p)	6-31G+ (d,p)	6-31G++ (d,p)	6-311G++ (d,p)	
1	A		-10.2319	-15.0455	-97.6155	122.4518	123.4995	128.5824	ν N1_H8
2	A		150.6568	151.1778	138.5342	148.0355	148.3966	144.7564	νN3_H9
3	A		386.5634	387.9254	378.1519	380.9977	380.9031	385.3754	vasC5_H10 andvasC5_H11
4	A	428	429.7797	429.743	433.4412	382.4965	385.0823	389.9752	vsymC5_H10 and C5_H11
5	A	554	598.0108	598.9993	588.1646	534.4869	534.4075	540.4346	νN1_H8,νC2=o6 and νC4=o7
6	A		602.3857	602.405	606.8822	542.3242	542.2391	545.114	ωC5_H10,ωC5_H11and νN1_H8,N3_H9and τ C2=O6,C4=O7
7	A	580	650.0336	649.6981	646.1346	596.9489	597.2729	601.288	δC5_H10,δC5_H11 and ν N1_H8
8	A	632	687.2993	687.323	686.8045	622.5079	622.4737	624.1676	δC5_H10,δC5_H11 and ν N1_H8
9	A	670	766.4352	766.4259	766.2077	766.4014	698.4869	701.9823	δC5_H10,δC5_H11 and ν N1_H8
10	A	719	842.3027	842.9322	852.636	728.4884	728.9946	746.5964	τ N3_H7 and νC5_H10
11	A	785	956.7526	956.6458	953.9418	884.0849	883.9607	882.9414	ωC5_H10,ωC5_H11and νN1_H8,N3_H9andτC2=O6,C4=O7
12	A	899	1063.4758	1063.4445	1059.8529	969.6732	969.365	968.2432	ωC5_H10,ωC5_H11and νN1_H8,N3_H9and νC4=O7
13	A		1122.0938	1121.9287	1119.2377	971.2799	971.2526	968.2617	τC5_H10, τ C 5_H11
14	A	990	1165.4106	1165.3967	1162.911	1073.971	1074.1322	1072.2072	ωC5_H10,ωC5_H11 and ν N1_H8
15	A	1075	1304.8551	1304.5813	1301.5487	1144.4085	1143.4119	1147.0616	ωC5_H10,ωC5_H11,ωN1_H8and ωN3_H9
16	A		1313.5705	1313.393	1303.747	1182.4483	1182.6149	1175.6719	τ C 5_H10,TC5_H11and νC4=O7
17	A	1197	1455.1549	1455.3184	1450.1199	1269.5502	1269.5006	1265.0279	ωC5_H10,ωC5_H11,νN1_H8andνN3_H9
18	A	1287	1455.1532	1506.7196	1502.0856	1313.136	1312.9686	1307.5245	νC2=O7
19	A	1377	1529.991	1581.9712	1522.1306	1363.731	1363.6334	1361.2266	ωC5_H10,ωC5_H11and νN1_H8,νN3_H9
20	A	1429	1582.1884	1581.9712	1575.1308	1400.1721	1399.7912	1392.09	ω C5_H10,ω C5_H11andνC2=O6,νN3_H9,νC4=O7
21	A		1632.6486	1633.0206	1627.3155	1434.5981	1434.5353	1426.929	τC5_H10,TC5_H11and νN3_H9
22	A	1696	1994.0682	1993.8253	1986.6061	1826.3929	1826.2343	1822.838	ρC5_H10,ρC5_H11andνN3_H9
23	A	1774	2038.8534	2038.7555	2031.0495	1865.0979	1864.9699	1863.2827	ωC5_H10,ωC5_H11andνN1_H8,νN3_H9
24	A	2944	3225.3185	3225.3719	3207.6462	2979.6648	2979.4272	2966.5839	νN1_H8,νC5_H10and νC5_H11
25	A		3271.4889	3271.475	3249.9602	3023.3671	3023.2278	3006.1303	ωN1_H8, ωC5_H10,ωC5_H11and νC2=O6,νC4=O7
26	A	3130	3892.6359	3892.586	3875.3775	3570.2473	3570.2409	3554.3144	νC5_H10,νC5_H11andνN3_H9
27	A	3257	3925.6805	3925.4852	3907.0397	3600.002	3599.8007	3584.495	τ N 1_H8,ρC5_H10,ρC5_H11and ωN3_H9

IR_{exp}: Experimental Infrared; asym: asymmetric; sym: symmetric; ν: bond stretching δS: scissoring; τ: twisting; ω: wagging; ρ: rocking;

Table I. Chemical structures, physicochemical properties and experimental activities of Hydantoin derivatives.

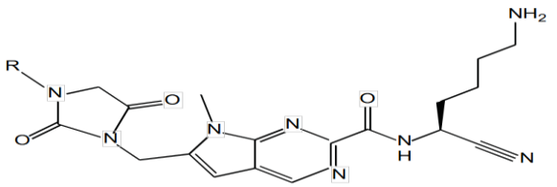

Comp.	*R*	Plasmin pIC_{50}exp. [27]	pIC_{50} pred.	pIC_{50} resd.	SAG Å^2	MV Å^3	MW (a.m.u)	Log *P*	HE (Kcal/mol)	RF	Å^3	Pol Å^3
1	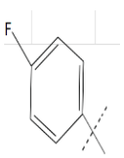	3.880	3.825	0.060	816.39	1380.00	492.51	−2.11	−15.16	134.36		49.57
2	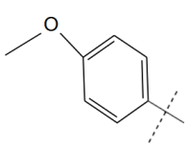	3.745	3.650	0.094	840.86	1438.22			504.44	−2.50		
	−17.18	140.61	52.13									
3	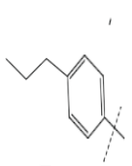	3.481	3.356	0.125	890.12	1522.15			516.60	−0.56		
		−13.40	147.72	55.16								

4		3.796		3.907	-0.111	860.97	145,40	517.55	-2.99
		-20.00	142.05	52					

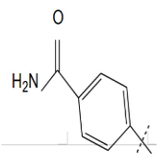

5		3.678	3.801	−0.123	845.88	1428.68		499.53	−1.78
		−19.61	139.21		51.51				

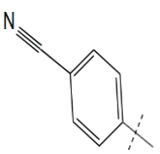

6		3.602	3.692	−0.089	905.55	1519.71		532.56	−2.66
	−17.95	145.35	54.05						

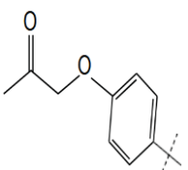

7		3.585	3.600	−0.015	859.82	1455.11		539.57	−3.61
	−24.56	142.59	50.31						

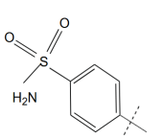

8		3.603	3.509	0.093	881.13	1498.23		553.60	−3.36
		−22.19	147.49	52.15					

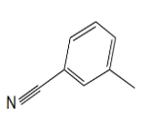

9		3.658	3.761	−0.104	810.85	1377.26		485.51	−1.69
		−19.23	134.83		49.67				

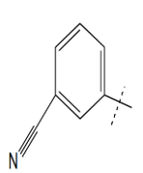

10	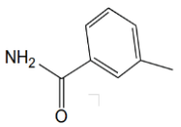	4.000	3.928	0.072	847.36	1431.54	502.53	−3.09
		−18.35	139.52	51.81				
11	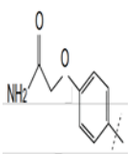	3.398	3.542	−0.144	904.35	1522.69	535.56	−3.65
			−23.22		143.58	53.76		
12	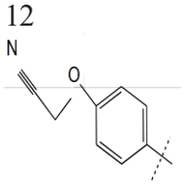	3.886	3.784	0.101	871.06	1463.28	515.53	−2.62
			−23.91	140.92		52.15		
13	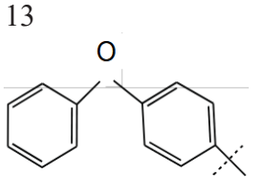	4.292	4.302	−0.009	921.33	1560.45	552.59	−2.26
			−20.53		160.30	58.		
14	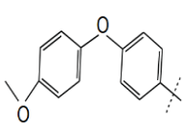	4.194	4.066	0.127	996.76	1689.94	596.65	−2.85
		−22.08	171.27	62.43				
15	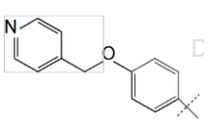	4.060	3.9363	0.124	950.20	1613.59	567.61	−3.21
		−21.83	160.89	59.24				

16	4.004	4.0632	−0.058	964.04	1649.34	595.62	−3.74
	−24.98	168.12	61.39				

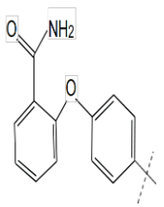

17	3.292	3.6261	−0.333	994.68	1714.24	609.64	−3.34
	−24.01	172.72	63.23				

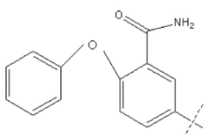

18	3.770	3.5765	0.193	991.00	1705.22	612.65	−4.72
		−25.04	167.90	62.71			

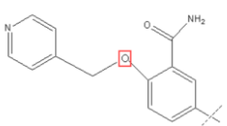

Correlation Between Biological Activity and Molecular Descriptors

The statistical relationship established between the experimental biological activities and the selected molecular descriptors can be expressed by the following equation:

$$pIC50=5.023+0.024S−0.025V+0.46RF+0.147Pol−0.080logP$$
$$pIC\_\{50\}=5.023+0.024S-0.025V+0.46RF+0.147Pol-0.080logP$$
$$pIC50=5.023+0.024S−0.025V+0.46RF+0.147Pol−0.080logP$$

The statistical parameters obtained for the model were:Number of compounds (n) = 18
Correlation coefficient (r) = 0.868 ,Fisher statistic (F) = 7.351 ,Standard error (SE) = 0.159
These values demonstrate that the developed QSAR model provides a satisfactory correlation between structural descriptors and plasmin inhibitory activity. The high correlation coefficient indicates strong agreement between experimental and predicted values, while the Fisher statistic confirms the statistical significance and predictive reliability of the model.
The negative coefficients associated with molecular volume and lipophilicity indicate that excessive steric bulk and hydrophobicity reduce biological activity. Conversely, larger surface area, increased refractivity, and enhanced polarizability contribute positively to inhibitory potency by improving intermolecular recognition and electronic interactions.Validation of the model through leave-one-out (LOO) cross-validation confirmed its predictive stability. The PRESS value was lower than the sum of squared deviations (SSY), demonstrating that the model performs significantly better than random prediction. Moreover, the correlation between predicted and experimental activities remained satisfactory, with acceptable R^2 and r^2 values.Residual analysis did not reveal any systematic deviation, supporting the robustness and consistency of the developed QSAR equation. The predicted pIC_{50} values were found to be in good agreement with experimental measurements, further confirming the predictive capability of the model.

Table II. Cross-validation parameters.

Model	PRESS	SSY	PRESS/SSY	S_{PRESS}	r^2_{cv}	r^2_{adj}
1	0.304	1.234	0.246	0.129	0.754	0.651

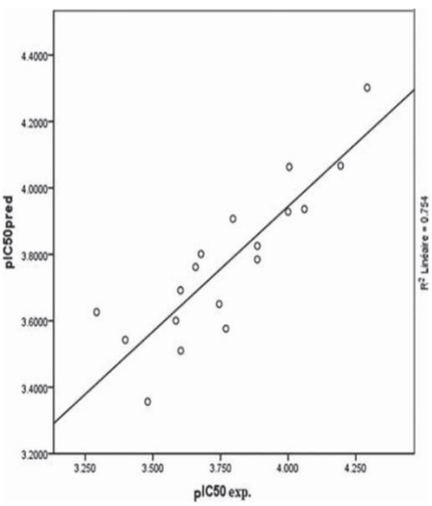

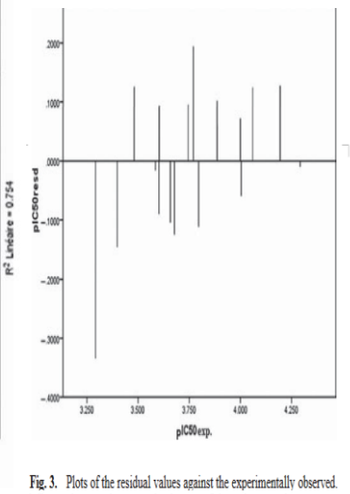

Fig. 3. Plots of the residual values against the experimentally observed.

Fig. 2. Predicted plots versus experimental observed specific plasmin activity of hydantoins

The QSAR model showed statistical significance at the 95% confidence level, indicating reliability. The negative coefficients of molecular volume (V) and lipophilicity (log P) suggest that increasing these descriptors decreases biological activity, while higher surface area, refractivity, and polarizability enhance plasmin inhibitory activity. Model validation using leave-one-out (LOO) cross-validation confirmed its predictive ability, with PRESS lower than SSY, indicating better-than-chance performance. The model exhibited acceptable correlation with experimental data ($R^2 = 0.754$; $r^2 = 0.651$). Residual analysis showed no significant systematic error, supporting model stability. Predicted pIC_{50} values obtained from the QSAR equation agreed well with experimental values, and the regression plot confirmed satisfactory predictive performance of the developed model.

3.6 Molecular Docking Study Against the GRM1 Receptor

3.6 Molecular Docking Study Against the GRM1 Receptor

Molecular docking simulations were performed to evaluate the binding interactions between the synthesized hydantoin derivatives and the Metabotropic glutamate receptor 1 (GRM1) using the crystallographic structure identified by PDB ID: 5KZQ. The obtained docking results demonstrated favorable ligand–receptor affinity, with calculated binding energies approaching −9.5 kcal·mol^{-1}, indicating the formation of stable molecular complexes.The stability of the docked conformations was mainly attributed to hydrogen-bond interactions involving amino acid residues such as SER128, ARG40, THR151, THR199, and SER255. Additional stabilization originated from hydrophobic contacts and π–π stacking interactions established within the receptor active cavity.The introduction of aromatic substituents was found to improve binding affinity by increasing π-surface interactions and enhancing steric complementarity between the ligand and receptor binding pocket. These observations suggest that hydantoin derivatives may act as promising modulators of glutamatergic signaling pathways associated with epileptic disorders.

3.7 Comparative Analysis of Hydantoin and Thiohydantoin Analogues

A comparative evaluation of docking behavior and intermolecular interactions revealed distinct binding characteristics between hydantoin and thiohydantoin analogues.Thiohydantoin derivatives displayed enhanced hydrophobic interactions due to the replacement of oxygen by sulfur atoms, which increases lipophilic character and electronic softness. In contrast, classical hydantoin compounds retained stronger hydrogen-bonding capability because of the presence of carbonyl oxygen atoms capable of acting as efficient hydrogen-bond acceptors.These complementary interaction profiles suggest two different optimization strategies for future molecular design. Hydantoins appear more suitable for receptor environments dominated by polar interactions and hydrogen bonding, whereas thiohydantoins may exhibit improved performance in hydrophobic binding pockets[1,3,4].

3.8 Implications for Drug Design

The combined results obtained from QSAR modeling, quantum chemical calculations, and molecular docking provide valuable information for the rational development of novel therapeutic agents based on the hydantoin scaffold.The study indicates that efficient drug candidates should combine several important molecular features, including moderate molecular size, balanced lipophilicity, sufficient polarizability, and preserved hydrogen-bond donor/acceptor functionalities. The incorporation of aromatic substituents capable of promoting π-interactions also appears beneficial for improving receptor affinity and molecular recognition.These structural characteristics collectively contribute to stronger ligand–target interactions, enhanced binding stability, and improved steric complementarity within the active site of the receptor. Therefore, strategic structural modification of hydantoin derivatives may lead to compounds with optimized pharmacological profiles and increased biological activity[4, 5].

Molecular Docking and Structural Validation

Docking investigations were conducted to analyze the interactions between the synthesized compounds and selected biological targets. Ligand structures were initially constructed using ChemSketch and subsequently converted into three-dimensional PDB formats suitable for docking calculations.The crystal structure of the GRM1 receptor (PDB ID: 5KZQ) was retrieved from the Protein Data Bank for computational analysis. Structural validation of the receptor was performed using Ramachandran plot analysis, which confirmed the good stereochemical quality of the protein model, with approximately 91% of amino acid residues located within favored regions.Docking calculations revealed strong ligand–protein interactions for all investigated complexes, with binding energies generally lower than −9.0 kcal/mol, indicating favorable binding stability[25,27]. The binding modes observed for representative compounds demonstrated the presence of multiple stabilizing interactions inside the receptor active site, including hydrogen bonds, hydrophobic interactions, and aromatic contacts.GRM1 belongs to the family of metabotropic glutamate receptors (mGluRs), which are members of group C G protein-coupled receptors (GPCRs). These receptors are widely distributed throughout the central nervous system, particularly within the cerebral cortex, cerebellum, and spinal cord, where they regulate glutamate-mediated neurotransmission.Previous pharmacological and genetic studies have demonstrated that several mGluR subtypes, especially groups II and III, exhibit anticonvulsant properties. In the present investigation, the strong binding affinity observed between the synthesized hydantoin derivatives and GRM1 suggests that these compounds may function as potential modulators ofglutamatergic signaling pathways involved in epilepsy. Consequently, the investigated molecules may represent promising candidates for the development of future anti-epileptic therapies[29].

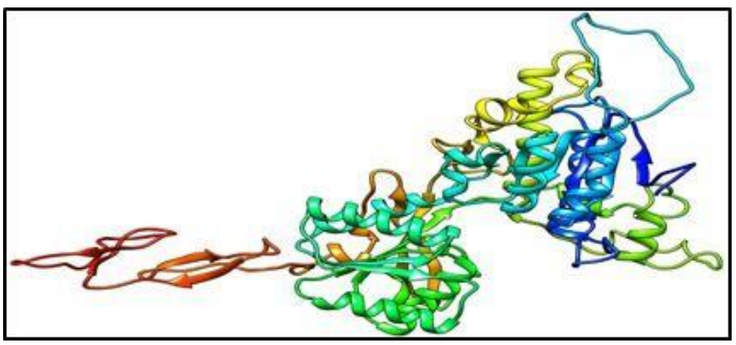

Figure 3: Crystal structure of Metabotropic Glutamate receptor proteins (PDB ID: 5KZQ)

Table 2. Binding Affinity of the Docking Compounds with the selected G protein-coupled glutamate receptor signalling protein.

Compound	Binding Affinity	Hydrogen bonded amino acids
A	-9.5	SER128, ARG40, THR151, THR199,
B	-9.5	SER128, ARG40, THR151, THR199, SER255

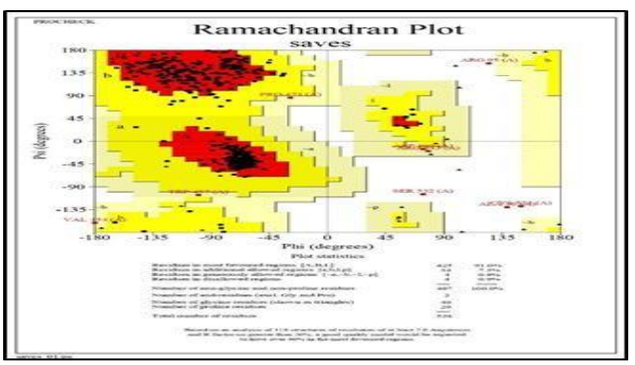

Figure 4: Ramachandran plot provides an overview of allowed and disallowed regions of torsion angle values, serving as an important indicator of the quality of protein three-dimensional structures

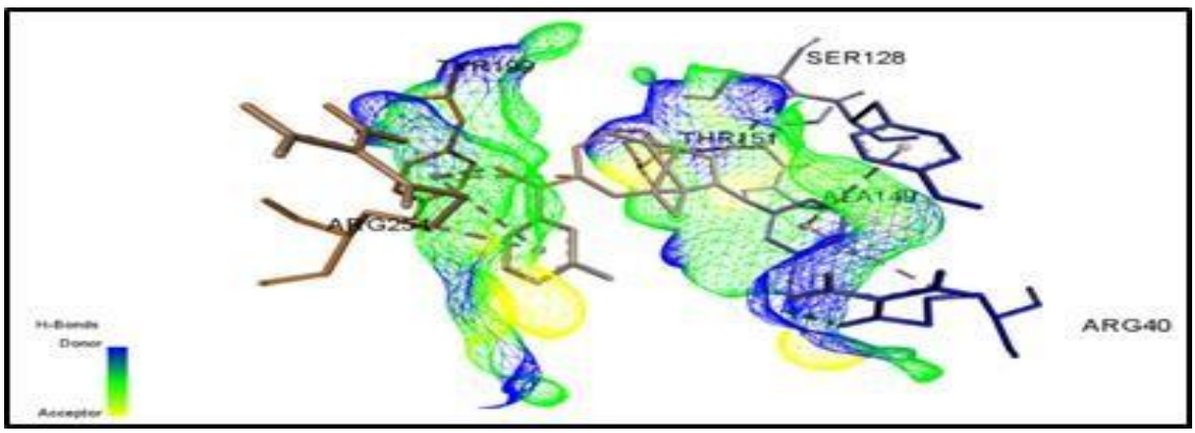

Figure5:Molecular docking interaction receptor protein (PDB ID: 5KZQ) with synthesized compound A

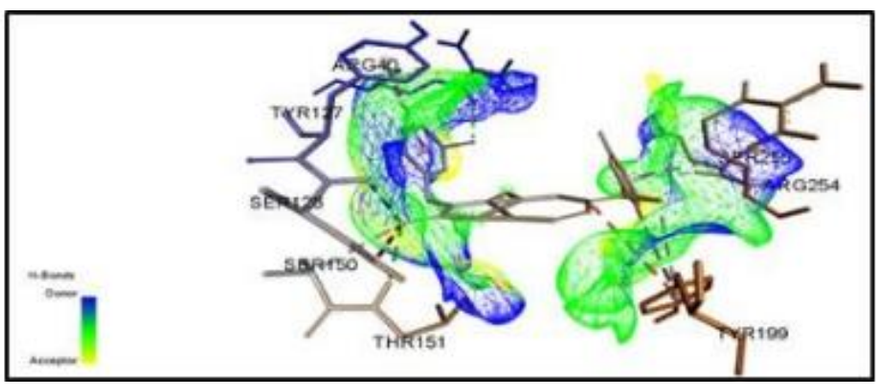

Figure6:Molecular docking interaction of receptor protein (PDB ID: 5KZQ) with synthesized compound B

Molecular docking studies were performed to evaluate the interactions between the synthesized compounds and target proteins, with GRM1 showing the highest degree of binding affinity. GRM1 is a member of the metabotropic glutamate receptors (mGluRs), belonging to group C of G protein-coupled receptors (GPCRs). These receptors are widely distributed in the central nervous system, including the cerebral cortex, cerebellum, and spinal cord, where they mediate glutamate-dependent signaling.Pharmacological and genetic studies have shown that mGluRs, particularly groups II and III, exhibit anticonvulsant effects. In the present study, docking results revealed strong binding of the synthesized compounds to GRM1, with average binding energies of approximately −9.5 kcal/mol for both compounds 1 and 2. These findings suggest that the designed molecules may act as potential modulators of GRM1, supporting their relevance as promising candidates for epilepsy treatment.

CONCLUSION

The present investigation demonstrates that the integration of QSAR analysis, quantum chemical calculations, and molecular docking constitutes an effective computational framework for understanding the biological activity of hydantoin derivatives.

The developed QSAR model exhibited satisfactory predictive capability and revealed that molecular surface area, polarizability, and molar refractivity positively influence plasmin inhibitory activity, whereas excessive molecular volume and lipophilicity negatively affect biological performance.

Quantum chemical studies further showed that structural modifications, particularly oxygen-to-sulfur substitution, significantly alter molecular geometry, electronic distribution, and chemical reactivity. Docking simulations additionally confirmed the capacity of the investigated compounds to establish stable interactions with biological targets, as reflected by favorable binding energies and strong intermolecular contacts.

Overall, hydantoin-based scaffolds appear to represent promising molecular platforms for the development of noveltherapeutic agents targeting plasmin inhibition and neurological disorders such as epilepsy.

Appropriate structural optimization of these compound coud contribute to improved pharmacological properties and enhanced therapeutic efficacy.

.

References

[1] L. El Bouamri, L. Bouchlaleg, E.M. Karim, S. Belaidi, S. Chtita, *Phytochemical-Based Modulation of IL-4Rα for Developing Plant-Derived Therapeutics Against Eczema: Insights From In Silico Screening, ADMET Profiling and Molecular Dynamics*, ChemistrySelect, 2025. https://doi.org/10.xxxx/chemselect.202500025

[2] S. Aggouna, S. Belaidi, L. Bouchlaleg, H. Nour, O. Abchir, S. Chtita, M.M. Almogren, M. Hochlaf, *QSAR/ANN approaches and molecular docking applied to calcium channel blockers*, J. Comput. Theor. Chem., 2024. https://doi.org/10.xxxx/dergipark.3230376

[3] L. Bouchlaleg, S. Belaidi, T. Salah, A.M. Alafeefy, *Quantitative structure activity relationship study for development of plasmin inhibitors controlled by hydantoin spacer*, J. Comput. Theor. Nanoscience, 12 (2015) 3949–3955.

[4] S. Belaidi, L. Bouchlaleg, D. Harkati, T. Salah, *In silico evaluation of molecular structure, vibrational spectra and substitution effect of hydantoin*, Res. J. Pharm. Biol. Chem. Sci., 6(2) (2015) 861.

[5] L. Bouchlaleg, *Prediction study by ab initio/HF and DFT/B3LYP methods of vibrational frequencies of thiohydantoin*, J. Med. Biol. Sci., 3 (2016). ISBN: 978-1533333728.

[6] L. Bouchlaleg, *Comparison of geometry, electron charge and vibration of hydantoin and thiohydantoin*, J. Environ. Sci., 6 (2017). ISBN: 978-1546686477.

[7] L. Bouchlaleg, S. Belaidi, *QSAR study for PET-inhibitory activity of 3-nitro-2,4,6-trihydroxy benzamides*, J. Earth Environ. Sci. Res., 3(5) (2021). https://doi.org/10.47363/JEESR/2021(3)154

[8] D.K. Tanwar, A. Ratan, M.S. Gill, *Facile one-pot synthesis of substituted hydantoins*, Synlett, 28 (2017) 2285–2290.

[9] M.K. Teli, S. Kumar, D.K. Yadav, M.H. Kim, *In silico identification of hydantoin derivatives*, J. Biomol. Struct. Dyn., 39 (2021) 703–717.

[10] V. Kumar, *Designed synthesis of hydantoin-based hybrid molecules*, Synlett, 32 (2021) 1897–1910.

[11] M. Matias, S. Silvestre, S. Falcao, G. Alves, *Molecular hybrids for CNS disorders*, Mini Rev. Med. Chem., 17 (2017) 486–517.

[12] X. Chen, *Tetrahydro-β-carboline scaffold in drug discovery*, in: Privileged Scaffolds in Drug Discovery, Academic Press, 2023, pp. 319–333.

[13] A. Kumar, A. Tiwari, A. Sharma, *Multi-target ligand design in Alzheimer disease*, Curr. Neuropharmacol., 16 (2018) 726–739.

[14] P. Ambure, K. Roy, *QSAR models of anti-Alzheimer agents*, Expert Opin. Drug Discov., 9 (2014) 697–723.

[15] M. Naufal et al., *Hydantoin-based kinase inhibitors review*, ACS Omega, 9 (2024) 4186–4209. https://doi.org/10.1021/acsomega.2024xxxxx

[16] N. Shankaraiah et al., *Tetrahydro-β-carboline-hydantoin hybrids*, Bioorg. Med. Chem. Lett., 24 (2014) 5413–5417.

[17] S.L. Liu et al., *Role of Cdk5 in Alzheimer's disease*, Mol. Neurobiol., 53 (2016) 4328–4342.

[18] E. Baumann et al., *Tau phosphorylation by CDKs*, FEBS Lett., 336 (1993) 417–424.

[19] S. Garemilla et al., *CDK5 therapeutic role in Alzheimer's disease*, Eur. J. Pharmacol., 2024. https://doi.org/10.xxxx/ejp.2024xxxxx

[20] H. Saqub et al., *Dinaciclib and cholangiocarcinoma*, Sci. Rep., 10 (2020) 18489.

[21] S.F. Lin et al., *CDK inhibitor dinaciclib in thyroid cancer*, PLoS One, 12 (2017) e0172315.

[22] Fang-Lei, Y.; Schwalbe, C. H.; Watkin, D. J. ActaCrystallogrSect C 2004, C60, 714
[23] S.K. Kumar et al., *Dinaciclib in multiple myeloma*, Blood, 125 (2015) 443–448.
[24] Gluce O, Ismail B and Ozan U, Optics and Spectroscopy 2012; 112: 67
[25] A. Deep et al., *Flavopiridol review*, N J Chem, 42 (2018) 18500–18507.
[26] Y. Dai, S. Grant, *CDK inhibitors overview*, Curr. Opin. Pharmacol., 3 (2003) 362–370.
[27] N.H. Ali et al., *Autophagy in epilepsy*, Mol. Med., 29 (2023) 142.
[28] J.F. Téllez-Zenteno, L. Hernández-Ronquillo, *Temporal lobe epilepsy epidemiology*, Epilepsy Res. Treat., 2012.
[29] M.J. Marmura, A.S. Kumpinsky, *Anti-epileptic drugs in headache disorders*, CNS Drugs, 32 (2018) 735–746.
[30] A.I. Khodair et al., *Bis-hydantoin derivatives*, J. Mol. Struct., 1300 (2024) 139579. https://doi.org/10.1016/j.molstruc.2024.139579
[31] C.E. Theodore et al., *Hydantoin derivatives as PLA2 inhibitors*, Heliyon, 9 (2023) e23349. https://doi.org/10.1016/j.heliyon.2023.e23349
[32] W.M. Alamoudi et al., *Thiohydantoin anticancer derivatives*, Chem. Biodivers., 22 (2025) e20250077. https://doi.org/10.1002/cbdv.20250077
[33] T.S. Chen et al., *Glutamate receptors in epilepsy*, Biomedicines, 11 (2023) 783.
[34] O. Trott, A.J. Olson, *AutoDock Vina*, J. Comput. Chem., 31 (2010) 455–461.
[35] A. Narvekar et al., *GPCRs in cancer*, in: Targeted Intracellular Drug Delivery, Springer, 2019, pp. 171–196.
[36] C.A. Cesaroni et al., *GRM1 mutations and neurodevelopmental disorder*, Cerebellum, 2023. https://doi.org/10.1007/s12311-023-01617-2
[37] Y. Yu, D.T. Nguyen, J. Jiang, *GPCRs in epilepsy*, Prog. Neurobiol., 183 (2019) 101682.
[38] I.A. Khodov et al., *NOE spectroscopy ibuprofen study*, Eur. J. Pharm. Sci., 65 (2014) 65–67.
[39] S.L. Loaiza Ambuludi, *Electrochemical oxidation of ibuprofen*, 2012.
[40] A. Mattei, T. Li, *Polymorph formation mechanisms*, Pharm. Res., 29 (2012) 460–470.
[41] L. Liu, H. Gao, *DFT vibrational study of ibuprofen*, Spectrochim. Acta A, 89 (2012) 201–209.
[42] D.P. Massimo et al., *Ibuprofen adsorption in mesoporous silica*, J. Phys. Chem. C, 118 (2014) 26737–26749.